Supporting Material

Mitochondrial energetics, pH regulation, and ion dynamics: A combined computational-experimental approach

An-Chi Wei[1], Miguel A. Aon[2], Brian O'Rourke[2], Raimond L. Winslow[1], Sonia Cortassa[1,2]

[1]Institute of Computational Medicine, Department of Biomedical Engineering, and [2]Division of Cardiology, School of Medicine, Johns Hopkins University, Baltimore, MD

Mitochondrial Model of Energy Metabolism and ion dynamics

The mitochondrial model developed in the present manuscript is based on the model published by Cortassa et al.(1, 2).The mitochondrial models accounts for the basic mitochondrial electrophysiology and energetics, including the TCA cycle, oxidative phosphorylation and ion transport across inner mitochondrial membrane. Succinate dehydrogenase (SDH) is now modeled as part of the respiratory chain in the mitochondria membrane. Two transporters, the mitochondrial Na^+/H^+ exchanger (NHE), and the mitochondrial phosphate carrier (PiC), were added to the original mitochondrial model. The mitochondrial concentrations of protons, sodium ions, and phosphate ions were added as new state variables. In the model formulation, the pH in the mitochondria matrix is not a constant, thus it is necessary to consider the pH effects on the ionic metabolite forms as well as its effects on the equilibrium constants. The new model formulation accounts for multiple equilibria for protons and magnesium with ATP, ADP, and phosphate. Also, apparent equilibrium constants of F_0F_1-ATPase, SDH, and succinate lyase(SL) are a function of pH. Besides the new components, we have adjusted the parameters in both TCA cycle and respiratory chain so that TCA cycle intermediate levels reproduced the literature data, and the temporal profile of mitochondrial NADH and membrane potential reproduce our experiments(Fig. 4 in the manuscript).The detailed mathematical expressions and parameters of the model are listed in the following sections.

Section 1.Computational modeling of Na^+/H^+ exchanger (NHE) and phosphate carrier (PiC)

Models of the Na^+/H^+ exchanger (NHE) and phosphate carrier (PiC) were developed and incorporated in the previous mitochondrial model. NHE, the main pathway of Na^+ efflux from mitochondria, was modeled using a two-state kinetic mechanism developed previously by Crampin and Smith(3).Model parameters were adjusted to ensure the reversibility of ion transport, as well as to match transport rates determined experimentally (4) (Fig. S1).

The steady state current through the NHE is described by the following equation:

$$J_{NHE} = c_{NHE} \frac{\dfrac{\beta_1^+ \beta_2^+ - \beta_1^- \beta_2^-}{\beta_1^+ + \beta_1^- + \beta_2^+ + \beta_2^-}}{1+10^{n_i(pH_i - pK_i)}} \qquad \text{(Eq.S1)}$$

where

$$\beta_1^+ = \frac{k_1^+ K_{H\_NHE}[Na^+]_m}{K_{H\_NHE}[Na^+]_m + K_{H\_NHE}K_{Na\_NHE} + K_{Na\_NHE}[H^+]_m}$$

$$\beta_2^+ = \frac{k_4^+ K_{Na\_NHE}[H^+]_i}{K_{H\_NHE}[Na^+]_i + K_{H\_NHE}K_{Na\_NHE} + K_{Na\_NHE}[H^+]_i}$$

$$\beta_1^- = \frac{k_1^- K_{H\_NHE}[Na^+]_i}{K_{H\_NHE}[Na^+]_i + K_{H\_NHE}K_{Na\_NHE} + K_{Na\_NHE}[H^+]_i}$$

$$\beta_2^- = \frac{k_4^- K_{Na\_NHE}[H^+]_m}{K_{H\_NHE}[Na^+]_m + K_{H\_NHE}K_{Na\_NHE} + K_{Na\_NHE}[H^+]_m}$$

being k_i^+ and k_i^-, pseudofirst order rate constants for the transition between different states with second order units (they are considered pseudo first order because only one of the two factors in the product in the rate expressions correspond to a state variable, e.g. H^+ or Na^+); K_{H_NHE} and K_{Na_NHE} are the dissociation constants of H^+ and Na^+.

The phosphate carrier mediates the electroneutral exchange of Pi and hydroxyl anion (OH^-) between mitochondrial and cytoplasmic compartments. Previous studies reported that two binding sites exist and form a ternary complex with Pi and OH^-, binding in a random order to either the mitochondrial or cytoplasmic side of PiC(5). Thus, PiC was modeled according to an equilibrium random Bi:Bi reaction kinetic scheme(6)whose steady state current is described by:

$$J_{PIC} = c_{PiC} \frac{V_{PIC,f}\frac{[H_2PO_4^{2-}]_i[OH^-]_m}{K_{Pi,i}K_{OH,m}} - V_{PIC,b}\frac{[H_2PO_4^{2-}]_m[OH^-]_i}{K_{Pi,m}K_{OH,i}}}{\left(1+\frac{[H_2PO_4^{2-}]_i}{K_{Pi,i}}+\frac{[OH^-]_m}{K_{OH,m}}+\frac{[H_2PO_4^{2-}]_m}{K_{Pi,m}}+\frac{[OH^-]_i}{K_{OH,i}}+\frac{[H_2PO_4^{2-}]_m[OH^-]_i}{K_{Pi,m}K_{OH,i}}+\frac{[H_2PO_4^{2-}]_i[OH^-]_m}{K_{Pi,i}K_{OH,m}}\right)} \quad \text{(Eq. S2)}$$

where $V_{PiC,f}$ and $V_{PiC,b}$ are the maximal forward and backward transport rates of PiC, respectively; $K_{Pi,i}$ and $K_{Pi,m}$ are the cytosolic and mitochondrial Pi dissociation constants, and $K_{OH,i}$ and $K_{OH,m}$ are the cytosolic and mitochondrial OH^-dissociation constants. The dissociation constants for Pi and OH^-were assumed to be the same at the inner and outer sites of the mitochondrial inner membrane. Figure S2 shows the Lineweaver-Burk representation of the PiC kinetics, and its simulation with Eq. S2. Model parameters for PiC are listed in Table S1.

Table S1. **Parameter values for the mitochondrial sodium proton exchanger and phosphate carrier**

Symbol	Value	Units	Description	Eq.	References
k_1^+	0.0252	ms^{-1}	NHE forward rate constant	1	adjusted
k_1^-	0.0429	ms^{-1}	NHE backward rate constant	1	adjusted
k_4^+	0.16	ms^{-1}	NHE forward rate constant	1	adjusted
k_4^-	0.0939	ms^{-1}	NHE backward rate constant	1	Constrained*
K_{Na_NHE}	24	mM	Na+Dissociation constant	1	(4)
pK_H	6.8		pKa value of dissociation constant for H+	1	(7)
pK_i	8.52		Proton inhibitory constant	1	(7)
n_i_NHE	3		Hill coefficient for H+ binding	1	(8)
c_{NHE}	0.28 (NHE) or 0.00785 (mitochondria)	mM	NHE concentration	1	adjusted
$K_{Pi,e}$	11.06	mM	ExtramitochondrialPi binding constant	2	(5)
$K_{Pi,m}$	11.06	mM	Mitochondrial Pi binding constant	2	(5)
$K_{OH,e}$	40.8	nM	Extramitochondrial OH- binding constant	2	(5)
$K_{OH,m}$	40.8	nM	Mitochondrial OH- binding constant	2	(5)
$V_{PiC,f}$	90	µmol min^{-1} mg $protein^{-1}$	Forward V_{max}	2	adjusted
$V_{PiC,b}$	90	µmol min^{-1} mg $protein^{-1}$	Backward V_{max}	2	adjusted
c_{PiC}	1(PiC) or 1.6915 (mitochondria)	mg protein ml^{-1}	PiC concentration	2	adjusted

* by microscopic reversibility

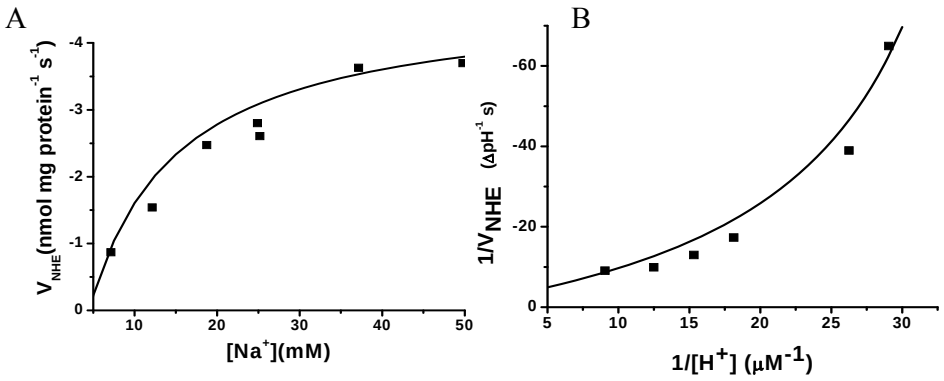

Figure S1. Model and experimental data illustrating the (A)Na_i and(B)pH_m dependence of the Na^+/H^+ exchanger (NHE) flux

The adjusted kinetic parameters for the NHE module were: K_{Na_NHE}= 24mM and pKm= 6.8, pKi=8.52; k_1^+ =0.0252 ms^{-1}, k_1^- =0.0429ms^{-1}, k_4^+ =0.160ms^{-1}, $k_4^- = k_1^+ k_4^+ / k_1^-$, n=3, NHE concentration =0.03.Data points correspond to experimental measurements (4) whereas the solid line corresponds to steady-state NHE flux obtained from the rate expression in Eq. S1. Panel A:Initial rates of H^+ efflux from rat heart mitochondria while external Na^+ concentration was varied (4). Simulation conditions were set to $[H^+]_i$=1.0 10^{-7}M, $[H^+]_m$=1.12 10^{-7}M, $[Na^+]_m$=5mM, $[Na^+]_i$= 5-50mM, NHE_conc=0.28mM. Panel B: Initial rates of H^+ efflux as a function of mitochondrial pH, pH_m, in the presence of antimycin A. After pH_m reached a steady state, 50mM Na_i was rapidly injected(4). Simulation conditions were set to $[H^+]_i$=1.0 10^{-7}M, $[H^+]_m$=1.12 10^{-7}M, $[Na^+]_m$=5mM, $[Na^+]_i$= 5~50mM. The units conversion used the proton buffering power of mitochondria reported in (4) (40nmol H^+/pH unit), and the mitochondrial NHE protein concentration was adjusted to reproduce the experimental data.

A B

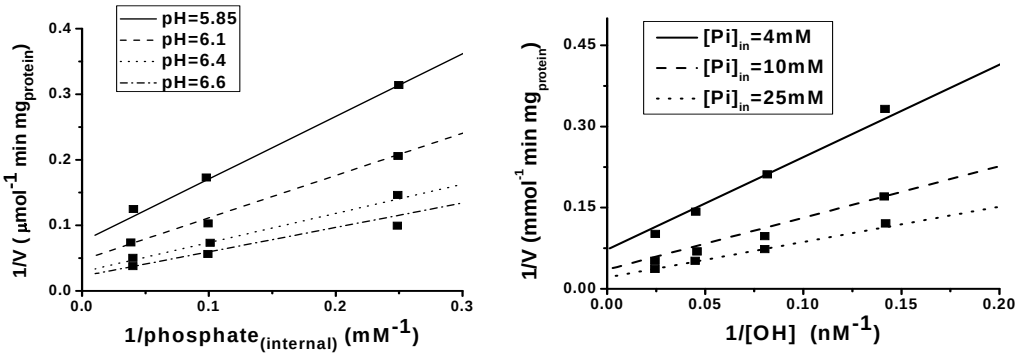

Figure S2.Model and experimental data of PiC fluxes

The plotscorrespond toLineweaver-Burk representations of experimental and computational data. Individual data points indicate experimental data whereas continuous lines correspond to the plot of the phosphate carrier rate expression (Eq. S2). (A)Initial rates of internal phosphate efflux are plotted as function of the internal phosphate concentrations from reconstituted mitochondrial membranes (5), at pH values 5.85, 6.1, 6.4, and 6.6 in the presence of valinomycin and nigericin; (B) Initial rates of internal phosphate efflux at pH conditions, corresponding to OH^- ion concentrations of 7.1, 12.6 and 39.8nM.

Section 2.TCA cycle

The optimization criterion for the TCA cycle kinetic parameters was provided by the intermediary concentrations reported by Randle and Tubbs (9)(Table S2). Those concentrations were simulated by the model under respiratory state 3 conditions at the steady state.

Table S2. **Adjustment of model parameters for the TCA cycle**

TCA cycle intermediate	Experimental data*	Model†
Citrate	**0.23**	**0.239**
Isocitrate	**0.03**	**0.054**
2-Oxoglutarate	**0.131**	**0.149**
SuccinylCoA	**0.0658**	**0.0308**
Succinate	**0.329**	**0.341**
Fumarate	**0.329**	**0.248**
Malate	**0.164**	**0.219**
Oxaloacetate	**0.023**	**0.0177**
Sum‡	**1.303**	**1.3**
AcCoA‡	**0.003-0.009**	**0.001-0.01**
NADH+NAD‡	**0.86**	**1**

* converted from(9)tomM units.

† simulated under respiratory state 3 conditions after 500 seconds.

‡ Model parameter adjusted according to experimental data.

Section 3. Ordinary differential equations of the mitochondrial model

TABLE S3. System of differential and algebraic equations used in the mitochondrial model

$\frac{d\Delta\Psi_m}{dt} = \frac{V_{He} + V_{He(SDH)} - V_{Hu} - V_{ANT} - V_{Hleak} - V_{NaCa} - 2V_{uni}}{C_{mito}}$	(S3)
$\frac{d\,[ADP]_m}{dt} = V_{ANT} - V_{ATPase} - V_{SL}$	(S4)
$[ATP]_m = C_A - [ADP]_m$	(S5)
$\frac{d[NADH]}{dt} = - V_{O2} + V_{IDH} + V_{KGDH} + V_{MDH}$	(S6)
$\frac{d[ISOC]}{dt} = V_{ACO} - V_{IDH}$	(S7)
$\frac{d[\alpha KG]}{dt} = V_{IDH} - V_{KGDH} + V_{AAT}$	(S8)
$\frac{d[SCoA]}{dt} = V_{KGDH} - V_{SL}$	(S9)
$\frac{d[Suc]}{dt} = V_{SL} - V_{O_2SDH}$	(S10)
$\frac{d[FUM]}{dt} = V_{O_2SDH} - V_{FH}$	(S11)
$\frac{d[MAL]}{dt} = V_{FH} - V_{MDH}$	(S12)
$\frac{d[OAA]}{dt} = V_{MDH} - V_{CS} - V_{AAT}$	(S13)
$[CIT] = \mathrm{C}_{\mathrm{Kint}} - \left(\begin{array}{r} [\mathrm{ISOC}] + [\alpha KG] + [SCoA] + [Suc] + \ldots \\ \ldots + [FUM] + [MAL] + [OAA] \end{array} \right)$	(S14)
$\frac{d[Ca^{2+}]_m}{dt} = \delta_{Ca}\left(V_{uni} - V_{NaCa}\right)$	(S15)
$\frac{d[Na^+]_m}{dt} = V_{NHE} - 3V_{NaCa}$	(S16)
$\frac{d[Pi]_m}{dt} = -V_{ATPase} + V_{PiC} - V_{SL}$	(S17)
$\frac{d[H^+]_m}{dt} = \delta_H \left(-\sum_i \overline{N}_H^i \frac{d[L_i]}{dt} - \sum_{k=1}^{N_r} n_k J_k + J_H \right)$	(S18)

Section 4. Rate equations

In the following sections we recapitulate all equations of the updated mitochondrial energetics model, irrespective of them being new to this upgrade or identical to the previous version of the model.

TCA cycle rate equations

$$V_{CS} = \frac{k_{cat}^{CS} E_T^{CS}}{\left(1+\frac{K_M^{AcCoA}}{[AcCoA]}\right)\left(1+\frac{K_M^{OAA}}{[OAA]}\right)}$$

$$V_{ACO} = k_f^{ACO}\left([CIT] - \frac{[ISOC]}{K_E^{ACO}}\right)$$

$$V_{IDH} = k_{cat}^{IDH} E_T^{IDH}\left[\begin{array}{l}\left(1+\frac{[H^+]_m}{k_{h,1}}+\frac{k_{h,2}}{[H^+]_m}\right)+ f_i^{IDH}\left(\frac{K_M^{NAD}}{[NAD]}\right)+\ldots \\ f_a^{IDH}\left(\frac{K_M^{ISOC}}{[ISOC]}\right)^{ni} + f_a^{IDH} f_i^{IDH}\left(\frac{K_M^{ISOC}}{[ISOC]}\right)^{ni}\left(\frac{K_M^{NAD}}{[NAD]}\right)\end{array}\right]^{-1}$$

$$f_a^{IDH} = \left[\left(1+\frac{[ADP^{3-}]_m}{K_{ADP}^a}\right)\left(1+\frac{[Ca^{2+}]_m}{K_{Ca}^a}\right)\right]^{-1}$$

$$f_i^{IDH} = \left(1+\frac{[NADH]}{K_{i,NADH}}\right)$$

$$V_{KGDH} = \frac{k_{cat}^{KGDH} k_T^{KGDH}}{1+\frac{[H^+]_m}{k_{h,1a}}+\frac{k_{h,2a}}{[H^+]_m}+ f_a^{KGDH}\left(\frac{k_M^{\alpha KG}}{[\alpha KG]}\right)^{n_{\alpha KG}} + f_a^{KGDH}\frac{k_M^{NAD}}{[NAD]}}$$

$$f_a^{KGDH} = \left[\left(1+\frac{[Mg^{2+}]}{K_D^{Mg^{2+}}}\right)\left(1+\frac{[Ca^{2+}]_m}{K_D^{Ca^{2+}}}\right)\right]^{-1}$$

$$V_{SL} = k_f^{SL}\left([SCoA][ADP]_m[Pi]_m - \frac{[Suc][ATP]_m[CoA]}{K_{E,app}^{SL}}\right)$$

$$K_{E,app}^{SL} = K_{Eq}^{SL}\frac{P_{SUC}P_{ATP}}{P_{Pi}P_{ADP}}$$

Succinate dehydrogenase is included in the respiratory complexes table

$$V_{FH} = k_f^{FH}\left([FUM] - \frac{[MAL]}{K_E^{FH}}\right)$$

$$V_{MDH} = \frac{k_{cat}^{MDH} E_T^{MDH} f_{h,a} f_{h,i}}{1 + \frac{K_M^{MAL}}{[MAL]}\left(1 + \frac{[OAA]}{K_i^{OAA}}\right) + \frac{K_M^{NAD}}{[NAD]} + \frac{K_M^{MAL}}{[MAL]}\left(1 + \frac{[OAA]}{K_i^{OAA}}\right)\frac{K_M^{NAD}}{[NAD]}}$$

$$f_{h,a} = \left(1 + \frac{[H^+]}{k_{h1}} + \frac{[H^+]^2}{k_{h1}k_{h2}}\right)^{-1} + k_{offset}$$

$$f_{h,i} = \left(1 + \frac{k_{h3}}{[H^+]} + \frac{k_{h3}k_{h4}}{[H^+]^2}\right)$$

$$V_{AAT} = k_f^{AAT}[OAA][GLU]\frac{k_{ASP}K_E^{ATT}}{\left(k_{ASP}K_E^{AAT} + [\alpha KG]k_f^{AAT}\right)}$$

$$V_{AAT} = K_f^{AAT}\left([OAA][GLU] - \frac{[\alpha KG][ASP]}{K_E^{AAT}}\right)$$

Oxidative Phosphorylation rate equations

$$V_{O_2} = 0.5\rho^{res}\frac{\left(r_a + r_{c1}e^{\left(\frac{6F\Delta\Psi_B}{RT}\right)}\right)e^{\left(\frac{FA_{res}}{RT}\right)} - r_a e^{\left(\frac{g6F\Delta\mu_H}{RT}\right)} + r_{c2}e^{\left(\frac{FA_{res}}{RT}\right)}e^{\left(\frac{g6F\Delta\mu_H}{RT}\right)}}{\left(1 + r_1 e^{\left(\frac{FA_{res}}{RT}\right)}\right)e^{\left(\frac{6F\Delta\Psi_B}{RT}\right)} + \left(r_2 + r_3 e^{\left(\frac{FA_{res}}{RT}\right)}\right)e^{\left(\frac{g6F\Delta\mu_H}{RT}\right)}}$$

$$V_{He} = 6\rho^{res}\frac{\left(r_a e^{\left(\frac{A_{res}F}{RT}\right)} - (r_a + r_b)e^{\left(\frac{g6F\Delta\mu_H}{RT}\right)}\right)}{\left(1 + r_1 e^{\left(\frac{FA_{res}}{RT}\right)}\right)e^{\left(\frac{6F\Delta\Psi_B}{RT}\right)} + \left(r_2 + r_3 e^{\left(\frac{FA_{res}}{RT}\right)}\right)e^{\left(\frac{g6F\Delta\mu_H}{RT}\right)}}$$

$$A_{res} = \frac{RT}{F}\ln\left(K_{res}\sqrt{\frac{[NADH]}{[NAD^+]}}\right)$$

$$V_{O_2SDH} = 0.5\rho^{res(SDH)}\frac{\left(r_a + r_{c1}e^{\left(\frac{4F\Delta\Psi_B}{RT}\right)}\right)e^{\left(\frac{FA_{RSDH}}{RT}\right)} - r_a e^{\left(\frac{g4F\Delta\mu_H}{RT}\right)} + r_{c2}e^{\left(\frac{FA_{RSDH}}{RT}\right)}e^{\left(\frac{g4F\Delta\mu_H}{RT}\right)}}{\left(1 + r_1 e^{\left(\frac{FA_{RSDH}}{RT}\right)}\right)e^{\left(\frac{4F\Delta\Psi_B}{RT}\right)} + \left(r_2 + r_3 e^{\left(\frac{FA_{RSDH}}{RT}\right)}\right)e^{\left(\frac{g4F\Delta\mu_H}{RT}\right)}}\left(\frac{1}{1 + \frac{[OAA]}{K_i^{OAA}}}\right)$$

$$V_{HSDH} = 4\rho^{res(SDH)}\frac{\left(r_a e^{\left(\frac{A_{RSDH}F}{RT}\right)} - (r_a + r_b)e^{\left(\frac{g4F\Delta\mu_H}{RT}\right)}\right)}{\left(1 + r_1 e^{\left(\frac{FA_{RSDH}}{RT}\right)}\right)e^{\left(\frac{4F\Delta\Psi_B}{RT}\right)} + \left(r_2 + r_3 e^{\left(\frac{FA_{RSDH}}{RT}\right)}\right)e^{\left(\frac{g4F\Delta\mu_H}{RT}\right)}}\left(\frac{1}{1 + \frac{[OAA]}{K_i^{OAA}}}\right)$$

$$A_{RSDH} = \frac{RT}{F}\ln\left(K_{RSDH,app}\sqrt{\frac{[SUC]}{[FUM]}}\right)$$

$$K_{RSDH,app} = \frac{K_{res(SDH)}}{P_{SUC}}$$

$$V_{ATPase} = -\rho^{F1}\frac{\left(100\,p_a + p_{c1}\exp(3F\Delta\Psi_B/RT)\right)\exp(A_{F1}F/RT) - \left(\begin{array}{l} p_a\exp(3F\Delta\mu_H/RT) \\ \cdots + p_{c2}\exp(A_{F1}F/RT)\exp(3F\Delta\mu_H/RT)\end{array}\right)}{\left(1+p_1\exp(A_{F1}F/RT)\right)\exp(3F\Delta\Psi_B/RT) + \left(p_2 + p_3\exp(A_{F1}F/RT)\right)\exp(3F\Delta\mu_H/RT)}$$

$$V_{Hu} = -3\rho^{F1}\frac{100\,p_a\left(1+\exp(A_{F1}F/RT)\right) - \left(p_a + p_b\right)\exp(3F\Delta\mu_H/RT)}{\left(1+p_1\exp(A_{F1}F/RT)\right)\exp(3F\Delta\Psi_B/RT) + \left(p_2 + p_3\exp(A_{F1}F/RT)\right)\exp(3F\Delta\mu_H/RT)}$$

$$A_{F1} = \frac{RT}{F}\ln(K_{app}^{ATPase}\frac{[MgATP^{2-}]}{[ADP_{free}][Pi_{total}]})$$

$$K_{app}^{ATPase} = K_{ref}^{ATPase}[H^+]^1\frac{P_{ATP}P_{H_2O}}{P_{ADP}P_{Pi}}$$

Acid-base equilibria of adenine nucleotides and phosphate

Chemical species in the biochemical reactions exist in mixed ionic forms such as protonated, deprotonated or binding to different cations(10-13). In general, the total concentration of ligand is the sum of free ligand, ligand bound to proton and to metals(13).

$$[L_{total}] = [L] + \sum_{P=1}^{N_P}[LH_P] + \sum_{m=1}^{N_m}[LM^m]$$

, where L is the ligand, H is the proton and M^m is the m^{th} metal ion.

Here, only the most abundant and physiological significant forms of ATP, ADP, and phosphate in the pH range from 5.0 to 9.0 were considered: ATP^{4-}, $HATP^{3-}$, $MgATP^{-}$, ADP^{3-}, $HADP^{2-}$, $MgADP^{-}$, HPO_4^{2-}, and $H_2PO_4^{-}$.

$$[ATP^{4-}]_m = \frac{[ATP_{total}]_m}{\left(1 + \frac{[H^+]_m}{K_{a,ATP}} + \frac{[Mg^{2+}]_m}{K_{Mg,ATP}}\right)}$$

$$[HATP^{3-}]_m = \frac{[ATP^{4-}]_m [H^+]_m}{K_{a,ATP}}$$

$$[MgATP^{2-}]_m = \frac{[ATP^{4-}]_m [Mg^{2+}]_m}{K_{Mg,ATP}}$$

$$[ADP^{3-}]_m = \frac{[ADP_{total}]_m}{\left(1 + \frac{[H^+]_m}{K_{a,ADP}} + \frac{[Mg^{2+}]_m}{K_{Mg,ADP}}\right)}$$

$$[HADP^{2-}]_m = \frac{[ADP^{3-}]_m [H^+]_m}{K_{a,ADP}}$$

$$[MgADP^{-}]_m = \frac{[ADP^{3-}]_m [Mg^{2+}]_m}{K_{Mg,ADP}}$$

$$[H_2PO_4^-]_m = \frac{[Pi]_{total}}{1 + \frac{[H^+]_m}{K_{a,Pi}}}$$

$$[HPO_4^{2-}]_m = \frac{[H_2PO_4^-]_m K_{a,Pi}}{[H^+]_m}$$

$$[ATP^{4-}]_i = \frac{[ATP_{total}]_i}{\left(1 + \frac{[H^+]_i}{K_{a,ATP}} + \frac{[Mg^{2+}]_i}{K_{Mg,ATP}}\right)}$$

$$[ADP^{3-}]_i = \frac{[ADP_{total}]_i}{\left(1 + \frac{[H^+]_i}{K_{a,ADP}} + \frac{[Mg^{2+}]_i}{K_{Mg,ADP}}\right)}$$

$$[ATP_{total}] = [ATP^{4-}] + [HATP^{3-}] + [MgATP^{-}]$$

$$[ATP_{free}] = [ATP^{4-}] + [HATP^{3-}]$$

$$[ADP_{free}] = [ADP^{3-}] + [HADP^{2-}]$$

$$[Pi_{total}] = [H_2Pi^-] + [H\ Pi^{2-}]$$

Polynomials for species undergoing acid-base equilibrium, ionic gradients, and conservation relations

$$P_{ATP} = 1 + \frac{[H^+]_m}{K_{a,ATP}} + \frac{[Mg^{2+}]_m}{K_{Mg,ATP}}$$

$$P_{ADP} = 1 + \frac{[H^+]_m}{K_{a,ADP}} + \frac{[Mg^{2+}]_m}{K_{Mg,ADP}}$$

$$P_{Pi} = 1 + \frac{[H^+]_m}{K_{a,Pi}}$$

$$P_{SUC} = 1 + \frac{[H^+]_m}{K_{a,SUC}}$$

$$P_{H_2O} = 1 + \frac{[H^+]_m}{K_{a,H_2O}}$$

$$\Delta\mu_H = -2.303\frac{RT}{F}\Delta pH + \Delta\Psi_m$$

$$\Delta pH = pH_i - pH_m$$

$$\Delta\Psi_m = \Psi_i - \Psi_m$$

$$[NAD^+] = C_{PN} - [NADH]$$

$$[ATP_{total}] = C_A - [ADP_{toal}]$$

Adenine Nucleotide translocator (ANT)

The rate expression of the ANT has been modified to better represent the dependence of the rate with respect to the cytoplasmic ADP concentration, as follows:

$$V_{ANT} = \mathrm{V}_{\mathrm{maxANT}} \frac{\left(1 - \frac{[ATP^{4-}]_i \times [ADP^{3-}]_m}{[ADP^{3-}]_i \times [ATP^{4-}]_m}\right)\exp(-F\Delta\Psi_m / RT)}{\left(1 + \frac{[ATP^{4-}]_i}{[ADP^{3-}]_i}\exp(-hF\Delta\Psi / RT)\right)\left(1 + \frac{[ADP^{3-}]_m}{[ATP^{4-}]_m}\right)}$$

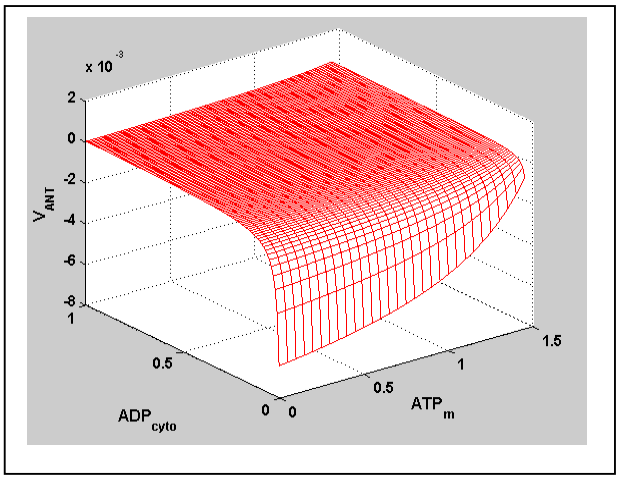

Figure S3. Dependence of ANT rate upon the concentration of cytoplasmic ADP, ADP_{cyto}, and mitochondrial ATP, ATP_m. Both variables are subjected to conservation relations being 1.0 for ADP+ATP in the cytoplasm, and 1.5 for ADP+ATP in the mitochondrial matrix. The expression is consistent with a reversion of the rate of ATP transport at low ADP_{cyto} and ATP_m.

Ionic fluxes rate equations

$$V_{uni} = V_{\max}^{uni} \frac{\frac{[Ca^{2+}]_i}{K_{trans}}\left(1+\frac{[Ca^{2+}]_i}{K_{trans}}\right)^3 \frac{2F\left(\Delta\Psi_m - \Delta\Psi^\circ\right)}{RT}}{\left(\left(1+\frac{[Ca^{2+}]_i}{K_{trans}}\right)^4 + \frac{L}{\left(1+\frac{[Ca^{2+}]_i}{K_{act}}\right)^{n_a}}\right)\left(1-e^{\left(\frac{-2F\left(\Delta\Psi_m-\Delta\Psi^\circ\right)}{RT}\right)}\right)}$$

$$V_{NaCa} = V_{\max}^{NaCa} \frac{e^{\left(\frac{bF\left(\Delta\Psi_m-\Delta\Psi^\circ\right)}{RT}\right)} e^{\left(\ln\frac{[Ca^{2+}]_m}{[Ca^{2+}]_i}\right)}}{\left(1+\frac{K_{Na}}{[Na^+]_i}\right)^n \left(1+\frac{K_{Na}}{[Ca^{2+}]_m}\right)}$$

$$J_{NHE} = c_{NHE} \frac{\frac{\beta_1^+\beta_2^+ - \beta_1^-\beta_2^-}{\beta_1^+ + \beta_1^- + \beta_2^+ + \beta_2^-}}{1+10^{n_i(pH_i - pK_i)}}$$

$$\beta_1^+ = \frac{k_1^+ K_{H\_NHE}[Na^+]_m}{K_{H\_NHE}[Na^+]_m + K_{H\_NHE}K_{Na\_NHE} + K_{Na\_NHE}[H^+]_m}$$

$$\beta_2^+ = \frac{k_2^+ K_{Na\_NHE}[H^+]_i}{K_{H\_NHE}[Na^+]_i + K_{H\_NHE}K_{Na\_NHE} + K_{Na\_NHE}[H^+]_i}$$

$$\beta_1^- = \frac{k_1^- K_{H\_NHE}[Na^+]_i}{K_{H\_NHE}[Na^+]_i + K_{H\_NHE}K_{Na\_NHE} + K_{Na\_NHE}[H^+]_i}$$

$$\beta_2^- = \frac{k_2^- K_{Na\_NHE}[H^+]_m}{K_{H\_NHE}[Na^+]_m + K_{H\_NHE}K_{Na\_NHE} + K_{Na\_NHE}[H^+]_m}$$

$$J_{PIC} = c_{PiC} \frac{V_{PIC,f}\frac{[HPO_4^{2-}]_i[OH^-]_m}{K_{Pi,i}K_{OH,m}} - V_{PIC,b}\frac{[HPO_4^{2-}]_m[OH^-]_i}{K_{Pi,m}K_{OH,i}}}{\left(1+\frac{[HPO_4^{2-}{}_i}{K_{Pi,i}} + \frac{[OH^-]_m}{K_{OH,m}} + \frac{[HPO_4^{2-}]_m}{K_{Pi,m}} + \frac{[OH^-]_i}{K_{OH,i}} + \frac{[HPO_4^{2-}]_m[OH^-]_i}{K_{Pi,m}K_{OH,i}} + \frac{[HPO_4^{2-}]_i[OH^-]}{K_{Pi,i}K_{OH,m}}\right.}$$

$$V_{Hleak} = g_H \Delta\mu_H$$

$$J_H = -V_{HNe} - V_{HSDH} + V_{hu} + V_{NHE} + V_{PiC} + V_{Hleak}$$

$$\sum_{k=1}^{N_r} n_k J_k = -(V_{IDH} + V_{KGDH} + V_{MDH} - V_{ATPase})$$

$$\sum \overline{N}_H^i \frac{d[L_i]}{dt} = \frac{[H^+]_m}{K_{a,ATP}P_{ATP}}\frac{d[ATP]_m}{dt} + \frac{[H^+]_m}{K_{a,ADP}P_{ADP}}\frac{d[ADP]_m}{dt} + \frac{[H^+]_m}{K_{a,Pi}P_{Pi}}\frac{d[Pi]_m}{dt} + \frac{[H^+]_m}{K_{a,SUC}P_{SUC}}\frac{d[SUC]_m}{dt}$$

$$\frac{d[H^+]_m}{dt} = \delta_H\left(-\sum_i \overline{N}_H^{L_i}\frac{d[L_i]}{dt} - \sum_{k=1}^{N_r} n_k J_k + J_H\right)$$

Section 5. Parameter values used in the simulations:
Tricarboxylic acid cycle

Symbol	Value	Units	Description
[AcCoA]	$1.\ 10^{-4}$-1.10^{-2}	mM	Acetyl CoA concentration
k_{cat}^{CS}	$7.841.\ 10^{-6}$	ms^{-1}	Catalytic constant of CS
E_T^{CS}	0.4	mM	Concentration of CS
K_M^{AcCoA}	0.0126	mM	Michaelis constant for AcCoA
K_M^{OAA}	$6.4\ 10^{-4}$	mM	Michaelis constant for OAA
$C_{k\,\mathrm{int}}$	1.3	mM	Sum of TCA cycle intermediates
k_f^{ACO}	$3.896.\ 10^{-6}$	ms^{-1}	Forward rate constant of ACO
K_E^{ACO}	2.22		Equilibrium constant of ACO
$K_{i,NADH}$	0.19	mM	Inhibition constant by NADH
k_{cat}^{IDH}	0.0264	ms^{-1}	Rate constant of IDH
E_T^{IDH}	0.109	mM	Concentration of IDH
$k_{h,1}$	$1.\ \ 10^{-5}$	mM	Inoization constant of IDH
$k_{h,2}$	$9.\ 10^{-4}$	mM	Inoization constant of IDH
K_M^{ISOC}	1.52	mM	Michaelis constant for isocitrate
n_i	2.0		Cooperativity for isocitrate
K_M^{NAD}	0.923	mM	Michaelis constant for NAD^+
K_{ADP}^a	0.62	mM	Activation constant by ADP
K_{Ca}^a	$5\ 10^{-4}$	mM	IDH activation constant for Ca^{2+}
E_T^{KGDH}	0.5	mM	Concentration of KGDH
k_{cat}^{KDGH}	0.000883	ms^{-1}	Rate constant of KGDH
k_{cat}^{KDGH}	30	mM	Michaelis constant for KGDH
$k_{h,1a}$	4.10^{-5}	mM	Ionization constant of KGDH
$k_{h,2a}$	7.10^{-5}	mM	Ionization constant of KGDH
$K_D^{Mg^{2+}}$	0.0308	mM	Activation constant for Mg^{2+}
$K_D^{Ca^{2+}}$	$1.5.10^{-4}$	mM	Activation constant for Ca^{2+}
K_M^{NAD}	38.7	mM	Michaelis constant for NAD
$n_{\alpha KG}$	1.2		Hill coefficient of KGDH for αKG
$[Mg^{2+}]_m$	0.4	mM	Mg^{2+} concentration in mitochondria
$[Mg^{2+}]_i$	1.0	mM	Mg^{2+} concentration in cytosol/buffer
k_f^{SL}	0.0014	$mM^{-1}ms^{-1}$	Forward rate constant of SL
K_E^{SL}	3.115		Equilibrium constant of the SL reaction
[CoA]	0.02	mM	Coenzyme A concentrations.
k_f^{FH}	0.000415	ms^{-1}	Forward rate constant for FH.
K_E^{FH}	1.0		Equilibrium constant of FH
k_{h1}	$1.131.10^{-5}$	mM	Ionization constant of MDH
k_{h2}	26.7	mM	Ionization constant of MDH
k_{h3}	$6.68.\ 10^{-9}$	mM	Ionization constant of MDH
k_{h4}	$5.62.\ 10^{-6}$	mM	Ionization constant of MDH
k_{offset}	$3.99.\ 10^{-2}$		Offset of MDH pH activation factor

k_{cat}^{MDH}	0.00621	ms^{-1}	Rate constant of MDH
E_T^{MDH}	0.154	mM	Total MDH enzyme concentration
K_M^{MAL}	1.493	mM	Michaelis constant for malate
K_i^{OAA}	0.031	mM	Inhibition constant for oxalacetate
K_M^{NAD}	0.2244	mM	Michaelis constant for NAD^+
[GLU]	$1.10^{-4} \sim 20$	mM	Glutamate concentration.
k_f^{AAT}	0.00107	ms^{-1}	Forward rate constant of AAT
K_E^{AAT}	6.6		Equilibrium constant of AAT
k_{ASP}	1.510^{-6}	ms^{-1}	Rate constant of aspartate consumption

Oxidative phosphorylation

Symbol	Value	Units	Description
r_a	$6.394.10^{-13}$	ms^{-1}	Sum of products of rate constants
r_b	$1.762.10^{-16}$	ms^{-1}	Sum of products of rate constants
r_{c1}	$2.656.10^{-22}$	ms^{-1}	Sum of products of rate constants
r_{c2}	$8.632.10^{-30}$	ms^{-1}	Sum of products of rate constants
r_1	$2.077.10^{-18}$		Sum of products of rate constants
r_2	$1.728.10^{-9}$		Sum of products of rate constants
r_3	$1.059.10^{-26}$		Sum of products of rate constants
ρ^{res}	$9.0.10^{-5}$-0.02779	mM	Concentration of electron carriers (respiratory complexes I-III-IV)
K_{res}	$1.35.10^{18}$		Equilibrium constant of respiration
$\rho^{res(SDH)}$	0.00124	mM	Concentration of electron carriers (respiratory complexes II-III-IV)
$\Delta\Psi_B$	50	mV	Phase boundary potential
g	0.85		Correction factor for voltage
$K_{res(SDH)}$	$5.765.10^{13}$		Equilibrium constant of SDH
p_a	$1.656.10^{-8}$	ms^{-1}	Sum of products of rate constants
p_b	$3.373.10^{-10}$	ms^{-1}	Sum of products of rate constants
p_{c1}	$9.651.10^{-17}$	ms^{-1}	Sum of products of rate constants
p_{c2}	$4.585.10^{-17}$	ms^{-1}	Sum of products of rate constants
p_1	$1.346.10^{-4}$		Sum of products of rate constants
p_2	$7.739.10^{-7}$		Sum of products of rate constants
p_3	$6.65.10^{-15}$		Sum of products of rate constants
ρ^{F1}	0.1076	mM	Concentration of F_1F_0-ATPase
K_{F1}	$1.71.10^6$		Equilibrium constant of ATP synthesis
$[Pi]_i$	1.75-3.0	mM	Inorganic phosphate concentration
C_A	1.5	mM	Total sum of adenine nucleotides
V_{maxANT}	0.4354	mM ms^{-1}	Maximal rate of the ANT
h^{ANT}	0.5		Fraction of $\Delta\Psi_B$
g_H	$3.0.10^{-8}$-5.10^{-5}	mM ms^{-1} mV^{-1}	Ionic conductance of the inner membrane
C_{PN}	1.0	mM	Total sum of pyridine nucleotides
C_{mito}	$1.812.10^{-3}$	mM mV^{-1}	Inner membrane capacitance

Mitochondrial Ca^{2+} handling

Symbol	Value	Units	Description
$V_{\max}^{uni}$	0.002459	mM ms^{-1}	V_{max}uniporter Ca^{2+} transport
$\Delta\Psi^{\circ}$	91	mV	Offset membrane potential
K_{act}	$3.8.10^{-4}$	mM	Activation constant
K_{trans}	0.019	mM	K_d for translocated Ca^{2+}
L	110.0		K_{eq} for conformational transitions in uniporter
n_a	2.8		Uniporter activation cooperativity
$V_{\max}^{NaCa}$	$9.33.10^{-5}$	mM ms^{-1}	V_{max} of Na^+/Ca^{2+} exchanger
b	0.5		$_{\Delta\Psi_m}$ dependence on Na^+/Ca^{2+} exchanger
K_{Na}	9.4	mM	Exchanger Na^{2+} constant
K_{Ca}	$3.75.10^{-4}$	mM	Exchanger Ca^{2+} constant
n	3.0		Na^+/Ca^{2+} exchanger cooperativity
δ_{Ca}	$3.0.10^{-4}$		Fraction of free $[Ca^{2+}]_m$

Mitochondrial H^+ and Na^+ handling

Symbol	Value	Units	Description
δ_H	1.10^{-5*}	dimensionless	mitochondria H^+ buffering capacity
$pK_{a,ADP}$	6.38		pKa of ADP dissociation constant
$pK_{a,ATP}$	6.48		pKa of ATP dissociation constant
$pK_{a,Pi}$	6.75		pKa of Pi dissociation constant
$pK_{Mg,ATP}$	4.19		pK of Mg^{2+}ATP dissociation constant
$pK_{Mg,ADP}$	3.25		pK of Mg^{2+}ADP dissociation constant
$pK_{a,SUC}$	5.2	dimensionless	pKa of succinate dissociation constant
K_{a,H_2O}	1.10^{-14}	M	dissociation constant for water
$[H^+]_i$	1.10^{-4}	mM	cytosolic H^+ concentration
$[Na^+]_i$	5.0	mM	cytosolic Na^+ concentration
$[Ca^{2+}]_i$	110^{-4}	mM	cytosolic Ca^{2+} concentration
[ADP]i	0.01~1.0	mM	cytosolic ADP concentration

*fromNyguyen(6) and Vaughan-Jones (8)

Section 6. State variables initial conditions

Symbol	Value	Units	Description
$[ADP]_m$	0.00406	mM	Mitochondrial ADP
[NADH]	$1.41.10^{-10}$	mM	Mitochondrial NADH
$\Delta\Psi_m$	154.95	mV	mitochondrial membrane potential
[ISOC]	0.00984	mM	Isocitrate
[αKG]	0.00354	mM	α-ketoglutarate
[SCoA]	0.01582	mM	Succinyl CoA
[Suc]	0.00179	mM	Succinate
[FUM]	0.11024	mM	Fumarate
[MAL]	0.10969	mM	Malate
[OAA]	1.03599	mM	Oxalacetate
$[H^+]_m$	$9.19.10^{-5}$	mM	Mitochondrial H^+
[Na+]m	5.85096	mM	Mitochondrial Na^+
[Pi]m	6.47248	mM	Mitochondrial Pi
[Ca2+]m	$5.56.10^{-5}$	mM	Mitochondrial Ca^{2+}

Section 7.Glossary

Symbol	Definition
$\overline{N}_H^i$	Average proton binding of i^{th} metabolite
n_k	Proton stoichiometry of the k^{th} reference reaction
v_j^k	Stoichiometric coefficient of species j in the k^{th} reference reaction
J_k	Flux of k^{th}reaction
J_H	Transport flux of proton
N_r	Number of chemical reactions
K_{ref}^k	Equilibrium constant of k^{th}reference reaction
K_{app}^k	Apparent equilibrium constant of k^{th} reaction
δ_H	Proton buffer capacity
δ_{Ca}	Calcium buffer capacity
αKG	α-ketoglutarate
ASP	Aspartate
CIT	Citric acid
F_1F_o-ATPase	Mitochondrial F_1F_0ATP synthase
FUM	Fumarate
IDH	Isocitrate dehydrogenase
ISOC	Iscocitrate
KGDH	α-ketoglutarate dehydrogenase
MAL	Malate
OAA	Oxalacetate
SCoA	Succinyl CoA

Suc	Succinate
TCA	Tricarboxylic acid cycle
V_{AAT}	Rate of aspartate amino transferase
V_{ACO}	Rate of aconitase
V_{ANT}	Rate of the adenine nucleotide transferase
$V_{ATPsynthase}$	Rate of the F_1F_0ATP synthase
V_{CS}	Rate of the citrate synthase
V_{FH}	Rate of the fumaratehydratase
V_{He}	Rate of proton transport driven by complex I, III, and IV
V_{HSDH}	Rate of proton transport driven by complex II, III and IV
V_{Hleak}	Rate of proton leak across the inner mitochondrial membrane
V_{Hu}	Rate of proton uptake via F_1F_0ATP synthase
V_{IDH}	Rate of isocitrate dehydrogenase
V_{KGDH}	Rate of alph-ketoglutarate dehydrogenase
V_{MDH}	Rate of malate dehydrogenase
V_{NaCa}	Rate of the mitochondrial Na^+/Ca^{2+} exchanger
V_{NHE}	Rate of the mitochondrial Na^+/H^+ exchanger
V_{O_2}	Oxygen consumption rate driven by complex I
V_{O_2SDH}	Oxygen consumption rate driven by complex II
V_{PiC}	Rate of the mitochondrial phosphate carrier
V_{SDH}	Rate of succinate dehydrogenase (complex II)
V_{SL}	Rate of succinate lyase
V_{uni}	Rate of Ca^{2+}uniporter in the mitochondrial inner membrane
G/M	Glutamate and malate
DNP	Dinitrophenol
CN	Cyanide
$\Delta\psi_m$	Electrical potential across the mitochondrial inner membrane
Δp	Proton motive force

Section 8.pH regulation in the mitochondria

To account for pH regulation, our present mitochondria model includes direct proton activation to the TCA cycle enzymes IDH, MDH and KGDH, the acid transporters NHE and PiC, and the proton pumps as well as apparent equilibrium constants and multiple equilibrium with protons. The principles of proton consumption or release by biochemical reactions occurred in the mitochondria and pH effects on equilibrium constants in this model was build upon the work of Alberty(14, 15) and the extended work by Vinnakota et al.(13).

Differential equation for $[H^+]_m$

The pH change of the mitochondria was accounted from the proton flux through a set of reactions including biochemical reactions in the mitochondria, and also proton transport across the membrane.

$$\frac{d[H^+]_m}{dt} = \delta_H \left(-\sum_i \overline{N}_H^{L_i} \frac{d[L_i]}{dt} - \sum_{k=1}^{N_r} n_k J_k + J_H \right)$$, where δ_H is the proton buffer capacity of the mitochondrial matrix.

The first component is from the pH changes due the proton binding of the metabolite L_i. We considered just metabolites ADP, ATP, phosphate and succinate. $\overline{N}_H^{L_i}$ is the average proton bound to metabolite L_i.

$$\overline{N}_H^L = \frac{\sum_{p=1}^{N_p} p[L\ H_p]}{[L_{total}]} = \frac{\sum_{p=1}^{N_p} p[LH_p]}{[L] + \sum_{p=1}^{N_p} p[LH_p] + \sum_{m=1}^{N_m} p[LM^m]}$$

The second component $\sum_{k=1}^{N_r} n_k J_k$ accounts for pH change due to consumption flux through reactions in which H^+ participate. n_k is the stoichiometry for proton consumption of a reference reaction (see definition below)(13).J_k is the flux through k^{th} biochemical reaction and N_r is the total number of protons participating in the biochemical reaction. Proton consumption stoichiometry could be expressed as:

$$\Delta_r N_H = \sum_{\text{product}} \overline{N}_H^{\text{product}} - \sum_{\text{reactant}} \overline{N}_H^{\text{reactant}} + n$$

Here, we assumed the changes of average proton binding to metabolite are small within the physiological pH range, omitted the difference between the average proton binding of the reactants and the products, and only considered n proton consumed or generated in the reference reactions (Table S4)).

The third component, $J_{H,}$ is the proton fluxes that contribute to the mitochondrial pH changes, including proton pumps, proton leak and proton transports through NHE and PiC.

Table S4. Reference reactions

Reference reaction is defined as the reaction in terms of the reference species of the metabolites as defined in (13).Reference species are defined as the most deprotonated form of the metabolites in the range of pH 5.0-9.0(13).

Enzyme	Reference reactions	n
Citrate synthase	$AcCoA+OAA^{2-}+H_2O \rightleftharpoons CIT^{3-}+CoASH+H^+$	-1
Aconitase	$CIT^{3-} \rightleftharpoons ICIT^{3-}$	0
Isocitrate dehydrogenase	$ICIT^{3-}+NAD^+ + H_2O \rightleftharpoons AKG^{2-} + NADH + HCO_3^- + H^+$	-1
α-ketoglutarate dehydrogenase	$AKG^{2-} + CoASH + NAD^+ + H_2O \rightleftharpoons HCO_3^- + SCoA^- + NADH + H^+$	-1
Succinyl-CoA synthetase	$SCoA^- + ADP^{3-} + HPO_4^{2-} \rightleftharpoons CoASH + SUC^{2-} + ATP^{4-}$	0
Succinate dehydrogenase	$SUC^{2-} + CoQ \rightleftharpoons QH_2 + FUM^{2-}$	0
Fumarase	$FUM^{2-} + H_2O \rightleftharpoons MAL^{2-}$	0
Malate dehydrogenase	$NAD^+ + MAL^{2-} \rightleftharpoons OAA^{2-} + NADH + H^+$	-1
ATP hydrolysis	$ATP^{4-}+H_2O \rightleftharpoons ADP^{3-}+HPi^{2-}+H^+$	-1
ATP synthase	Reverse reaction of ATP hydrolysis	+1

Apparent equilibrium constant as a function of pH

Apparent equilibrium constant is defined in terms of the species concentration at equilibrium and a function of pH(13).

$$K' = [H^+]^n \frac{K_{ref} \prod P_{product}}{\prod P_{reactant}}$$

where n is proton stoichiometry of the reference reaction and P is the binding polynomial ($P=1+\sum_{P=1}^{N_P}\frac{[H]^P}{\prod_{l=1}^{P}K_{a,l}}+\sum_{m=1}^{N_m}\frac{[M^m]}{K_{M^m}}$). K_{ref} is the equilibrium constant for the reference reaction ($K_{ref}=e^{-\Delta_r G^0/RT}$).

In the model, equilibrium constants of the reactions of FoF1-ATPase, succinate dehydrogenase(SDH) and succinyl CoA lyase(SL) are considered as function of pH. In other reactions, the pH effect on the apparent equilibrium constant is assumed to be small enough to be neglected.

pH-dependence of TCA cycle enzyme activities

pH affects enzyme activities because the ionizable groups in the active sites of enzymes must be in the proper ionic form to maintain the catalytic function. The TCA cycle enzyme alpha-ketoglutarate dehydrogenase (KGDH),was modeled as a function of pH(16, 17) besides the other two enzymes isocitrate dehydrogenase (IDH), and malate dehydrogenase(MDH) in the TCA cycle. The mathematical expression of KGDH is described below with enzyme activities sensitive to pH (Fig.S4 A), Ca^{2+} (Fig.S4 B) and Mg^{2+}. The dissociation constants of protons and calcium were obtained by fitting to experimental data(18-20).

$$V_{KGDH}=\frac{k_{cat}^{KGDH}k_T^{KGDH}}{1+\frac{[H^+]_m}{k_{h,1a}}+\frac{k_{h,2a}}{[H^+]_m}+f_a^{KGDH}\left(\frac{k_M^{\alpha KG}}{[\alpha KG]}\right)^{n_{\alpha KG}}+f_a^{KGDH}\frac{k_M^{NAD}}{[NAD]}}$$

$$f_a^{KGDH}=\left[\left(1+\frac{[Mg^{2+}]}{K_D^{Mg^{2+}}}\right)\left(1+\frac{[Ca^{2+}]_m}{K_D^{Ca^{2+}}}\right)\right]^{-1}$$

(A) (B)

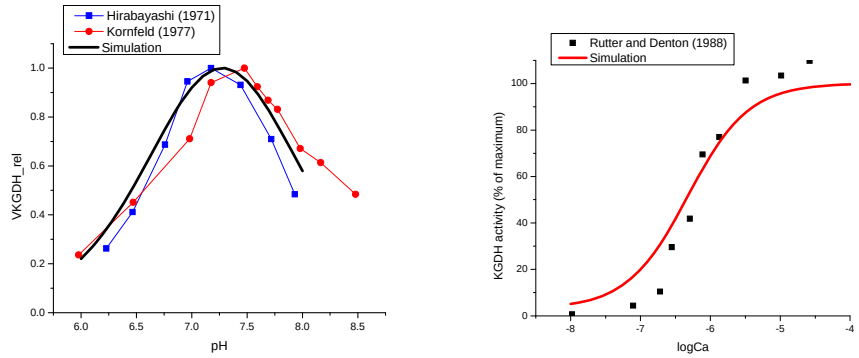

Figure S4. Model and experimental data of KGDH
(A) relative enzyme activity as a function of pH(18, 19) and (B) enzyme activity as a function of calcium(20).

Section 9.Experimental flow force relations in oxidative phosphorylation.

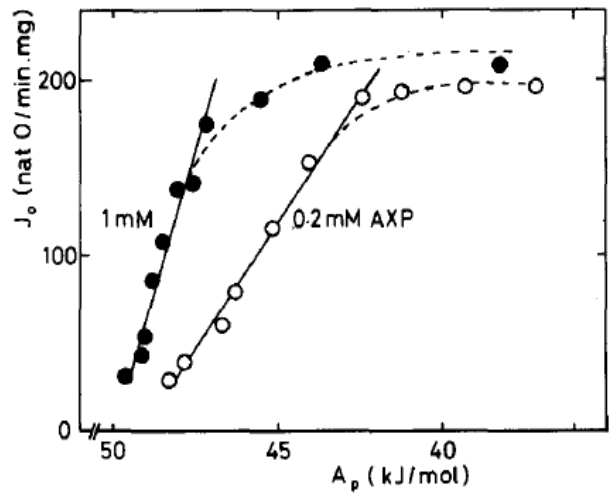

Figure S5. Relationship between mitochondrial oxygen uptake and affinity of phosphorylation with its dependence on the total adenine nucleotide concentration. Mitochondria were incubated with 20 mM succinate and hexokinase at different levels of sodium ATP: 0.2 mM (empty symbols) or 1.0 mM (filled symbols). Hexokinase will render various steady state levels of ATP/ADP and the large excess of succinate will ensure constant oxidation potential. Reproduced from van der Meer et al. (21).

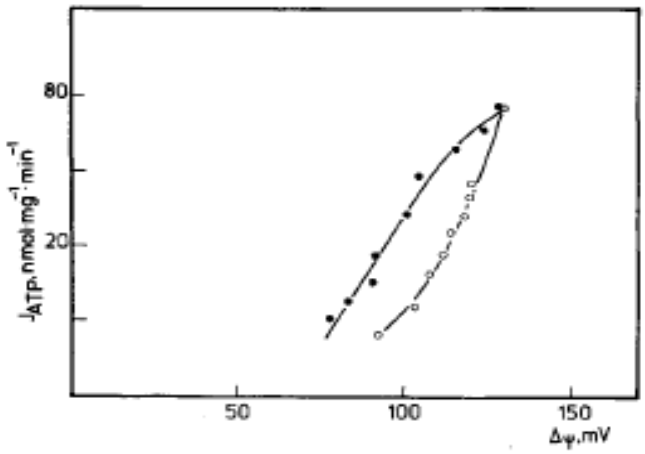

Figure S6.Relationship between succinate-driven J_{ATP} and membrane potential in titrations with FCCP and ClO_4^- . The measurements were carried out with mitochondrial particles in the presence of excess glucose and NADP, hexokinase and glucose 6 phosphate dehydrogenase. Filled symbols indicate titration with ClO_4^- whereas empty symbols depict titrations with FCCP. Reproduced from Petronilli et al.(22).

References

1. Cortassa, S., et al., *An integrated model of cardiac mitochondrial energy metabolism and calcium dynamics.*Biophys J, 2003. **84**(4): p. 2734-55.
2. Cortassa, S., et al., *A computational model integrating electrophysiology, contraction, and mitochondrial bioenergetics in the ventricular myocyte.*Biophys J, 2006. **91**(4): p. 1564-89.
3. Crampin, E.J. and N.P. Smith, *A dynamic model of excitation-contraction coupling during acidosis in cardiac ventricular myocytes.*Biophys J, 2006. **90**(9): p. 3074-90.
4. Kapus, A., E. Ligeti, and A. Fonyo, *Na+/H+ exchange in mitochondria as monitored by BCECF fluorescence.*FEBS Lett, 1989.**251**(1-2): p. 49-52.
5. Stappen, R. and R. Kramer, *Kinetic mechanism of phosphate/phosphate and phosphate/OH- antiports catalyzed by reconstituted phosphate carrier from beef heart mitochondria.* J BiolChem, 1994. **269**(15): p. 11240-6.
6. Nguyen, M.H., S.J. Dudycha, and M.S. Jafri, *Effect of Ca2+ on cardiac mitochondrial energy production is modulated by Na+ and H+ dynamics.* Am J Physiol Cell Physiol, 2007.**292**(6): p. C2004-20.
7. Brierley, G.P., et al., *Kinetic properties of the Na+/H+ antiport of heart mitochondria.*Biochemistry, 1989.**28**(10): p. 4347-54.
8. Vaughan-Jones, R.D., et al., *Intrinsic H(+) ion mobility in the rabbit ventricular myocyte.*J Physiol, 2002.**541**(Pt 1): p. 139-58.
9. Randle, P.J. and P.K. Tubbs, *Carbohydrate and fatty acid metabolism*, in *Handbook of Physiology*, R.M. Berne, N. Sperelakis, and R. Geiger, Editors. 1979, American Physiology Society. p. 805-844.
10. Alberty, R.A., *Thermodynamics of biochemical reactions*. 2003, Hoboken, N.J.: Wiley-Interscience. ix, 397 p.
11. Kushmerick, M.J., *Multiple equilibria of cations with metabolites in muscle bioenergetics.* Am J Physiol, 1997.**272**(5 Pt 1): p. C1739-47.
12. Alberty, R.A., *Biochemical Thermodynamics: Applications of Mathematica.* 2006.
13. Vinnakota, K., M.L. Kemp, and M.J. Kushmerick, *Dynamics of muscle glycogenolysis modeled with pH time course computation and pH-dependent reaction equilibria and enzyme kinetics.*Biophys J, 2006. **91**(4): p. 1264-87.
14. Alberty, R., *Thermodynamics of biochemical reactions*. 2003. ix, 397 p.
15. Alberty, R., *Biochemical Thermodynamics: Applications of Mathematica.* 2006.
16. Cornish-Bowden, A., *Fundamentals of enzyme kinetics*. 2004, Portland press.
17. Segel, I.H., *Enzyme kinetics: behavior and analysis of rapid equilibrium and steady state enzyme systmes*. 1993: Wiley & Sons.
18. Hirabayashi, T. and T. Harada, *Isolation and properties of -ketoglutarate dehydrogenase complex from baker's yeast (Saccharomyces cerevisiae).*BiochemBiophys Res Commun, 1971.**45**(6): p. 1369-75.

19. Kornfeld, S., M. Benziman, and Y. Milner, *Alpha-ketoglutarate dehydrogenase complex of Acetobacterxylinum. Purification and regulatory properties.* J BiolChem, 1977. **252**(9): p. 2940-7.
20. Rutter, G.A. and R.M. Denton, *Regulation of NAD+-linked isocitrate dehydrogenase and 2-oxoglutarate dehydrogenase by Ca2+ ions within toluene-permeabilized rat heart mitochondria. Interactions with regulation by adenine nucleotides and NADH/NAD+ ratios.*Biochem J, 1988. **252**(1): p. 181-9.
21. Van der Meer, R., H. Westeroff, and K. Van Dam, *Linear relation between rate and thermodynamic force in enzyme-catalyzed reactions.*BiochimBiophysActa, 1980.**591**(2): p. 488-493.
22. Petronilli, V., et al., *Flow-force relationships during energy transfer between mitochondrial proton pumps.*BiochimBiophysActa, 1991.**1058**(2): p. 297-303.